

[α /Fe] Patterns of Stars In The Halo Of The Galaxy

Young Sun Lee^{*a}, Timothy C. Beers^a, Daniela Carollo^b, and Thirupathi Sivarani^c

†

^a*Department of Physics & Astronomy, CSCE: Center for the Study of Cosmic Evolution, and JINA: Joint Institute for Nuclear Astrophysics, Michigan State University, East Lansing, MI 48824, USA*

^b*Research School of Astronomy and Astrophysics, The Australian National University, Weston, ACT 2611, Australia and INAF-Osservatorio Astronomico di Torino, Italy*

^c*Department of Astronomy, University of Florida, Gainesville, FL 32611, USA*
lee@pa.msu.edu, beers@pa.msu.edu, carollo@mso.anu.edu.au,
thirupat@astro.ufl.edu

A method for determining the abundance ratio of the α -elements (O, Mg, Si, Ca, Ti) with respect to Fe (collectively parameterized as “[α /Fe]”) from medium-resolution ($R = 2000$) spectra is explored. Results of a comparison with the ELODIE spectral library and from a noise injection experiment suggest that an accuracy in [α /Fe] of about 0.1 dex for spectra with $S/N \geq 20/1$ is achievable. This technique is used to estimate [α /Fe] for a total of 39,167 spectrophotometric and telluric calibration stars from the most recent public release of the Sloan Digital Sky Survey, in order to study the α -abundance patterns in stars of the Galactic halo. Local space velocities (U , V , W) and orbital parameters (such as Z_{\max} , R_{apo} , R_{peri} , V_{ϕ} , and eccentricity) are calculated for this sample, and a total of 7590 potential halo stars are selected by applying cuts of $V_{\phi} \leq 80 \text{ km s}^{-1}$, $Z_{\max} \geq 1 \text{ kpc}$, and $[\text{Fe}/\text{H}] \leq -1.0$. The sample is further divided into two groups: a dissipative component (or inner halo) with stars having $40 \leq V_{\phi} \leq 80 \text{ km s}^{-1}$ and $R_{\text{apo}} < 16 \text{ kpc}$ and an accreted component (or outer halo) with stars having $V_{\phi} < 40 \text{ km s}^{-1}$ and $R_{\text{apo}} \geq 16 \text{ kpc}$. Preliminary results for the comparison of the α abundance of these two samples are presented as a first step toward understanding the assembly history of the halos of the Galaxy.

*10th Symposium on Nuclei in the Cosmos
July 27 - August 1 2008
Mackinac Island, Michigan, USA*

*Speaker.

†We would like to acknowledge support from grant PHY 02-16783; Physics Frontier Center/Joint Institute for Nuclear Astrophysics (JINA), awarded by the U.S. National Science Foundation.

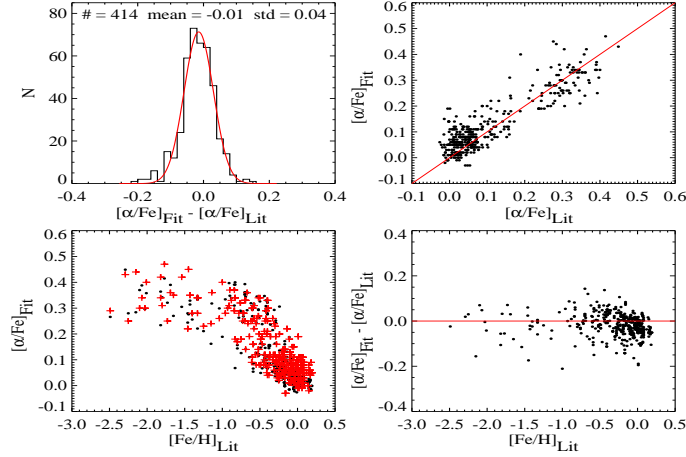


Figure 1: Comparison of [α /Fe] from our estimates (Fit) with those from the literature (Lit). The red crosses in the bottom left panel are our determinations.

1. Introduction

A recent study by Carollo et al. (2007) [1] has confirmed that the halo of the Milky Way is clearly divisible into at least two components – an inner and an outer halo. They show that the outer halo population exhibits a net retrograde rotation between -40 and -70 km s^{-1} (a more recent analysis puts this velocity at -85 km s^{-1}) and a peak in its metallicity distribution at $[\text{Fe}/\text{H}] = -2.2$, while the inner halo population consists of stars on net prograde orbits (between 0 and 50 km s^{-1}) with the metallicity peak at $[\text{Fe}/\text{H}] = -1.6$. They suggest that the outer halo formed through the assembly of smaller subsystems. If that is the case, the outer halo stars may possess different chemical signatures (e.g., low [α /Fe]) than the inner halo stars (e.g., high [α /Fe]) due to the lower star formation rate in the progenitors of the outer halo.

In this study, after developing a method for estimating [α /Fe] (the mean of [O/Fe], [Mg/Fe], [Si/Fe], [Ca/Fe], and [Ti/Fe]), we determine [α /Fe] for the sample of Carollo et al. ([1], Carollo et al., in prep). With the derived [α /Fe], which is often used as an indicator of tracing the star formation and chemical enrichment history of the Galaxy and its known satellite galaxies (e.g., [2]), we compare the α -abundance patterns between the inner and the outer halo.

2. Determination and Validation of [α /Fe]

In order to estimate [α /Fe] in an efficient manner for a large number of stars, we have generated a grid of synthetic spectra, using the Kurucz NEWODF models [3] and the TURBOSPECTRUM synthesis code [4]. The grid spans $4000 \text{ K} \leq T_{\text{eff}} \leq 8000 \text{ K}$ in steps of 250 K , $1.0 \leq \log g \leq 5.0$ in steps of 0.2 dex , $-3.0 \leq [\text{Fe}/\text{H}] \leq 0.2$ in steps of 0.2 dex , and $-0.1 \leq [\alpha/\text{Fe}] \leq 0.6 \text{ dex}$, in steps of 0.1 dex . We determine [α /Fe] using reduced χ^2 values obtained from matches of the observed spectra to this grid.

We have compared our [α /Fe] determination with that of 414 stars in the ELODIE spectral library [5] as a validation test. Figure 1 shows the results of the comparison. A Gaussian fit to the residuals between our values and those from the literature indicate that there is little systematic

POS(NIC X)213

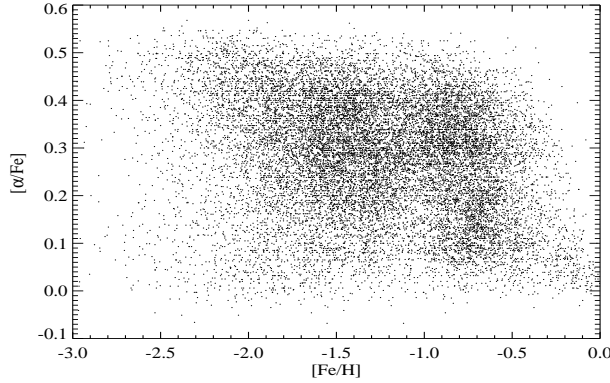


Figure 2: [α /Fe] as a function of [Fe/H] for 17450 stars.

offset, and further indicates a very small scatter (standard deviation of 0.04 dex). No trends in the estimated α -abundance as a function of [Fe/H] are noted for stars with [Fe/H] < -0.5 in the figure.

We also have checked how the S/N of a spectrum impacts our determination of the α -abundance, using a set of noise-added high-resolution calibration stars discussed in detail by [6]. From this experiment, we have obtained Gaussian means of -0.022, -0.016, -0.010, -0.006, and -0.005 and standard deviations of 0.092, 0.075, 0.057, 0.047, and 0.041 for $S/N = 15/1$, $20/1$, $30/1$, $40/1$, and $50/1$, respectively, from the residuals between spectra before and after noise injection. These results indicate that no significant offsets, and only a small standard deviation (< 0.1 dex) are found down to $S/N \sim 15/1$. However, in our analysis of the α -abundance patterns we only consider stars with $S/N \geq 20$.

3. Sample Selection and its Kinematic Parameters

Our program stars are the spectrophotometric and reddening standards from Data Release 6 of the Sloan Digital Sky Survey [7]. A detailed description on the selection of the sample stars and computation of the kinematic and orbital parameters of the sample can be found in [1]. Among the 39,167 calibration stars with U , V , W , R_{apo} , R_{peri} , V_{ϕ} , Z_{max} , e (eccentricity) calculated, about 20,000 stars with well-measured parameters in the range $T_{\text{eff}} = 5000 - 7000$ K have been selected. Since we only consider stars with $S/N \geq 20$, this yields 17,450 stars. Figure 2 plots [α /Fe] as a function of [Fe/H] for those stars.

To study the α -abundance patterns for stars in the Galactic halo, we impose three additional selection criteria: (1) $V_{\phi} \leq 80 \text{ km s}^{-1}$, which is more than 2σ ($2 \times 39 \text{ km s}^{-1}$) away from the typical thick-disk velocity ellipsoid centered on $V_{\phi} = 180 \text{ km s}^{-1}$ [8], (2) $[\text{Fe}/\text{H}] \leq -1.0$, and (3) $Z_{\text{max}} \geq 1 \text{ kpc}$. Applying these conditions to the total sample of 17,450 stars allows us to assemble 7580 stars with a high probability of halo membership. Following a scheme similar to [9], we further divide the halo sample into two sub-samples, and inner halo (or dissipative component) consisting of stars with $V_{\phi} \geq 40 \text{ km s}^{-1}$ and $R_{\text{apo}} < 16 \text{ kpc}$, and an outer halo (or accreted component) composed of stars with $V_{\phi} < 40 \text{ km s}^{-1}$ and $R_{\text{apo}} \geq 16 \text{ kpc}$. Even though it is understood that some overlap of these components surely exists after such a division, the cuts at 40 km s^{-1} and 16 kpc provides an adequate number of stars for both groups.

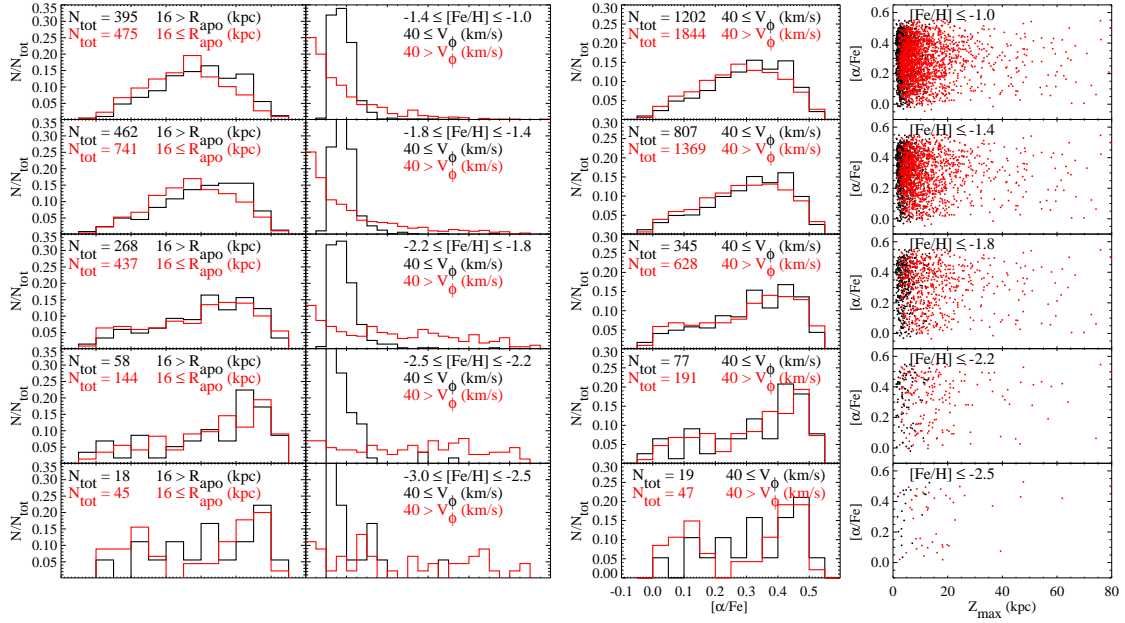


Figure 3: The two left panels are the distributions of [α /Fe] (left) and R_{peri} (right) with different bins of [Fe/H] for the inner (black) and outer (red) halo. The two right panels are the distribution of [α /Fe] (left) and Z_{max} (right), but cumulative over [Fe/H] as listed at the top of each panel.

4. Preliminary Results

The two left hand panels of Figure 3 show the fractional distribution of [α /Fe] and R_{peri} for various metallicity regimes of the dissipative component (in black) and the accreted component (in red). The metallicity cuts used to make the histograms is listed in the top legend of each right-hand panel. The prominent pattern that can be noticed in the left-hand panels of the figure is that as the cut on [Fe/H] decreases, the fractional number of stars with intermediate α -abundance (~ 0.25 dex) is reduced, whereas that of the low (below 0.2 dex) and high (above 0.3 dex)- α stars is increasing, implying a bifurcation of the population in a given metallicity range. It appears that this pattern occurs for the inner halo stars, too, although the outer halo stars exhibit a more conspicuous feature at the low metallicity end. This behavior is more apparent in the third column panels in the figure, which are the cumulative histograms over the [Fe/H] cuts. It is clear from the peaks of the α -abundance distribution in the two top left-hand panels that the outer halo stars have, on average, lower [α /Fe] with a larger scatter than the inner halo stars for the range [Fe/H] > -1.8 , confirming the claims of previous studies ([10, 9]). Below [Fe/H] = -1.8 , the difference in the mean [α /Fe] values between the two components disappears, owing to the much larger scatter in the [α /Fe] distribution.

In the histograms of the second-column panels shown in Figure 3, it can be seen that most of the inner halo stars with [Fe/H] > -2.2 are clustered at R_{peri} less than 3 kpc, with a small spread. Below this metallicity, the fraction of high R_{peri} stars increases; the scatter in R_{peri} becomes larger as well. A more salient feature in the distribution of R_{peri} can be seen for the outer halo stars in the histograms, which exhibit a much flatter distribution as [Fe/H] decreases. Since it is thought that if stars possess a common set of kinematics they are likely to share a common origin, the presence

of multiple (and different) features in the kinematics within one group in the narrow range of the metallicity may indicate a mixture of diverse populations, possibly including accreted stars from external systems.

The two right-hand panels plot the cumulative histograms (left) of [α /Fe] and α distribution versus Z_{\max} for the metallicity cuts listed at the top of each panel. On these plots, most of the metal-rich ([Fe/H] > -1.8) inner halo stars are concentrated at high α (> 0.25 dex), which is well-described by a standard Galactic halo evolution picture (that is, α -enhancement from SNe II). On the other hand, because large scatter in [α /Fe] is seen at the low metallicity end, the metal-poor ([Fe/H] < -1.8) inner halo stars might have formed through stochastic star formation at early times, supporting inhomogeneous Galactic chemical evolution models e.g., [11]), but contradicting other recent results (e.g., [12, 13]). The fact that most of the metal-poor outer halo stars have $Z_{\max} > 5$ kpc in the outer-most right hand panels gives support for the external origin as claimed by [1].

References

- [1] Carollo, D., et al. 2007, *Two stellar components in the halo of the Milky Way*, *Nature*, **450**, 1020
- [2] Geisler, D., et al. 2007, *Chemical Abundances and Kinematics in Globular Clusters and Local Group Dwarf Galaxies and Their Implications for Formation Theories of the Galactic Halo*, *PASP*, **119**, 939
- [3] Castelli, F., & Kurucz, R.L. 2003, *New Grids of ATLAS9 Model Atmospheres*, *IAUS*, **210**, p. A20
- [4] Alvarez, R., & Plez, B. 1998, *Near-infrared narrow-band photometry of M-giant and Mira stars: models meet observations*, *A&A*, **330**, 1109
- [5] Moultaqa, J., et al. 2004, *The ELODIE Archive*, *PASP*, **116**, 693
- [6] Lee, Y.S., et al. 2008, *The SEGUE Stellar Parameter Pipeline. I. Description and Comparison of Individual Methods*, *AJ*, in press [arXiv:0710.5645]
- [7] Adelman-McCarthy, J.K., et al. 2008, *The Sixth Data Release of the Sloan Digital Sky Survey*, *ApJS*, **175**, 297
- [8] Soubiran, C., Bienayme, O., & Siebert, A. 2003 *Vertical distribution of Galactic disk stars. I. Kinematics and metallicity*, *A&A*, **398** 141
- [9] Gratton, R.G., et al., *Abundances for metal-poor stars with accurate parallaxes. II. alpha -elements in the halo*, *A&A*, **406**, 131
- [10] Nissen, P.E., & Schuster, W.J. 1997, *Chemical composition of halo and disk stars with overlapping metallicities*, *A&A*, **326**, 751
- [11] Argast, D., et al. 2000, *Metal-poor halo stars as tracers of ISM mixing processes during halo formation*, *A&A*, **356** 873
- [12] Arnone, E., et al. 2005, *Mg abundances in metal-poor halo stars as a tracer of early Galactic mixing*, *A&A*, **430**, 507
- [13] Cayrel, R., et al. 2004, *First stars V - Abundance patterns from C to Zn and supernova yields in the early Galaxy*, *A&A*, **416**, 1117